Published in final edited form as:

Circ Res. 2020 May 08; 126(10): 1363–1378. doi:10.1161/CIRCRESAHA.119.316141.

PTH/PTHrP Receptor Signaling Restricts Arterial Fibrosis in Diabetic LDLR−/− Mice by Inhibiting Myocardin-Related Transcription Factor Relays

Abraham Behrmann[1,†], **Dalian Zhong**[1,†], **Li Li**[1,†], **Su-Li Cheng**[1], **Megan Mead**[1], **Bindu Ramachandran**[1], **Parastoo Sabaeifard**[1], **Mohammad Goodarzi**[2], **Andrew Lemoff**[2], **Henry M. Kronenberg**[3], **Dwight A. Towler**[1]

[1]Internal Medicine – Endocrine Division, UT Southwestern Medical Center, Dallas, TX 75390

[2]Biochemistry, UT Southwestern Medical Center, Dallas, TX 75390

[3]Endocrine Unit, Massachusetts General Hospital & Harvard Medical School, Boston, MA 02114

Abstract

Rationale: The PTH/PTHrP receptor (PTH1R) is expressed in vascular smooth muscle (VSM), and increased VSM PTH1R signaling mitigates diet-induced arteriosclerosis in LDLR−/− mice.

Objective: To study the impact of VSM PTH1R deficiency, we generated mice SM22-Cre:PTH1R(fl/fl);LDLR−/− mice (PTH1R-VKO) and Cre-negative controls (CON).

Methods and Results: Immunofluorescence and western blot confirmed PTH1R expression in arterial VSM that was reduced by Cre-mediated knockout. PTH1R-VKO cohorts exhibited increased aortic collagen accumulation in vivo, and VSM cultures from PTH1R-VKO mice elaborated more collagen (2.5-fold; p = 0.01) with elevated *Col3a1* and *Col1a1* expression. To better understand these profibrotic responses, we performed mass spectrometry on nuclear proteins extracted from CON and PTH1R-VKO VSM. PTH1R deficiency reduced Gata6 but upregulated the MADS-box transcriptional co-regulator, myocardin-related transcription factor A (Mkl1). Co-transfection assays (*Col3a1* promoter - luciferase reporter) confirmed PTH1R –mediated inhibition and Mkl1-mediated activation of *Col3a1* transcription. Regulation mapped to a conserved hybrid $CT(A/T)_6GG$ MADS-box cognate in the *Col3a1* promoter. Mutations of C/G's in this motif markedly reduced *Col3a1* transcriptional regulation by PTH1R and Mkl1. Upregulation of *Col3a1* and *Col1a1* in PTH1R-VKO VSM was inhibited by siRNA targeting *Mkl1*, and by treatment with

Address correspondence to: Dr. Dwight A. Towler , J.D. and Maggie E. Wilson Distinguished Chair in Biomedical Research, UT Southwestern Medical Center, Internal Medicine – Endocrine Division, 5323 Harry Hines Blvd, Dallas, TX 75390-8857 , Tel: (214) 648-2982, Dwight.Towler@utsouthwestern.edu.
[†]These authors contributed equally to the manuscript.

DISCLOSURES

D.A.T. has been approached as a consultant for new osteoporosis medications, but has not received remuneration.

SUPPLEMENTAL MATERIALS

Expanded Materials & Methods
Online Figures I – XXIV
Online Tables I – I
Major Resources Table
References[67–73]

the Mkl1 antagonist CCG1423 or the Rock2 inhibitor KD025. Chromatin precipitation demonstrated that VSM PTH1R deficiency increased Mkl1 binding to *Col3a1 and Col1a1,* but not *TNF,* promoters. Proteomic studies of plasma extracellular vesicles (EV) and VSM from PTH1R-VKO mice identified C1r and C1s, complement proteins involved in vascular collagen metabolism, as potential biomarkers. VSM C1r protein and *C1r* message were increased with PTH1R deficiency, mediated by Mkl1-dependent transcription and inhibited by CCG1423 or KD025.

Conclusions: PTH1R signaling restricts collagen production in the VSM lineage in part via Mkl1 regulatory circuits that control collagen gene transcription. Strategies that maintain homeostatic VSM PTH1R signaling, as reflected in EV biomarkers of VSM PTH1R/Mkl1 action, may help mitigate arteriosclerosis and vascular fibrosis.

Graphical Abstract

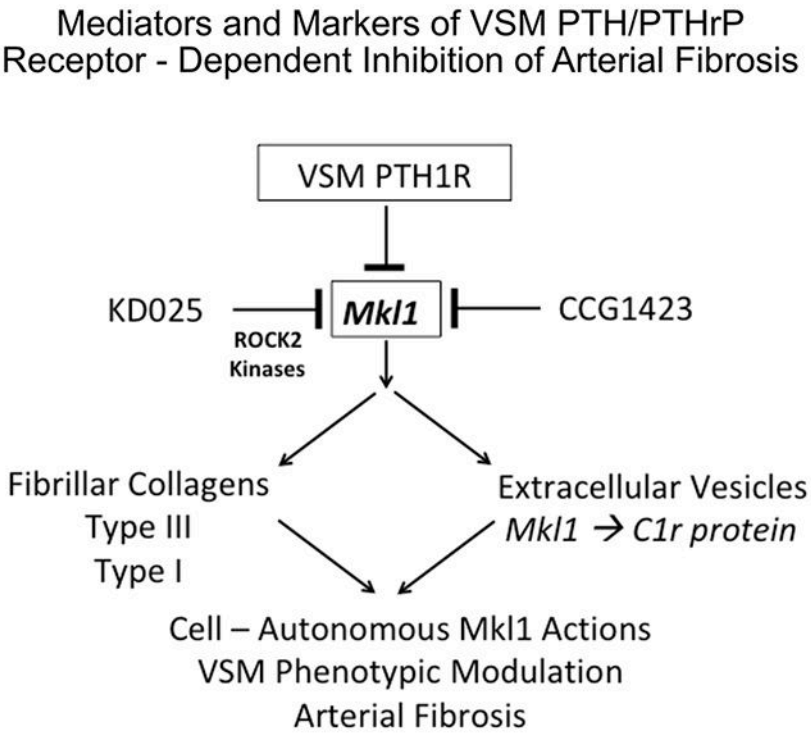

Keywords

Arteriosclerosis; collagen; vascular fibrosis; cardiovascular disease; myocardin-like protein; myocardin-related transcription factor; serum response factor; myocyte enhancer factor; metabolic syndrome; mass spectrometry; Animal Models of Human Disease; Cell Signaling / Signal Transduction; Fibrosis; Genetically Altered and Transgenic Models; Vascular Disease

INTRODUCTION

Arteriosclerosis and vascular fibrosis are pathobiological responses to conduit vessel inflammation, elicited by metabolic and mechanical insults that accrue with aging, lifestyle,

and genetic diathesis[1–3]. Hyperglycemia, hyperlipidemia, hypertension, and hyperphosphatemia are key contributors to arteriosclerotic disease biology. The metabolic syndrome – type 2 diabetes spectrum, either in the presence or absence of renal insufficiency, currently represents the most common clinical setting in which arteriosclerosis arises prematurely with age[4]. Studies by our group[1] and others[5–9] have shown that osteofibrogenic regulatory programs, similar to those that control bone formation, are ectopically activated the macrovasculature in response to diet-induced diabetes and dyslipidemia[1, 9]. As the molecular regulation of arterial osteofibrogenic matrix metabolism is revealed, pharmacologic or biologic strategies targeting these pathways afford therapeutic strategies to mitigate arteriosclerosis and its end-organ consequences (e.g. stroke, cognitive impairment, heart failure, myocardial infarction, renal insufficiency).

We previously demonstrated that (a) intermittent agonist-dependent activation or (b) transgene-mediated augmentation of vascular signaling via the receptor for parathyroid hormone (PTH) and PTH-related protein (PTHrP) suppressed aortic calcification, fibrosis and stiffness in a diet-induced arteriosclerosis model[10]. The PTH/PTHrP receptor, also known as PTH1R, regulates calcium phosphate homeostasis by conveying responses to its prototypic calciotropic ligands in the skeleton and in kidney tubules[11]. The PTH1R is also normally expressed in the cardiovascular system during development[12]. Global PTH1R deficiency in the mouse causes prenatal lethality due to cardiomyocyte apoptosis[12]. Diminished PTH1R activity also results in abnormal aortic valve morphogenesis[13]. In patients with mild primary hyperparathyroidism – a state of elevated circulating PTH that can induce PTH1R desensitization in VSM[14] –cardiovascular mortality risk is increased 2.7 fold[15]. In patients with primary hyperparathyroidism that warrants surgical intervention (age < 50, significant hypercalcemia, osteoporosis, renal insufficiency, and/or nephrolithiasis), surgical cure improves coronary flow reserve[16] and flow-mediated arterial responses[17]. Thus, the PTH1R plays important roles in cardiovascular biology[18].

To better understand the role of endogenous VSM PTH1R signaling in arteriosclerosis, we bred mice possessing floxed PTH1R alleles[19] with SM22-Cre transgenic mice[20] to conditionally delete the PTH1R in the VSM lineage. Since male LDLR−/−[21] mice develop diet-induced obesity, diabetes, and arteriosclerosis on high fat diet[22], comparison of SM22-Cre:PTH1R(fl/fl):LDLR−/− with PTH1R(fl/fl);LDLR−/− control siblings affords the opportunity to evaluate how VSM PTH1R deficiency impacts diet-induced disease. We find that VSM PTH1R limits vascular fibrosis and fibrillar collagen gene expression, mediated in large part via the inhibition of myocardin-related transcription factor -A (Mrtfa or Mkl1[23]) relays. We identify that, with VSM PTH1R deficiency, circulating extracellular vesicles (EVs) possess increased C1 complement proteins [24, 25] and reduced osteogenic signaling potential -- indicating that EV characteristics may prove useful for quantifying VSM PTH1R/Mkl1 signaling in health and disease.

METHODS

Major resources, methods, and supporting data are provided in online supplements.

The authors declare that all supporting data are available within the article and its online supplementary files. Any additional background information of interest concerning murine reagents, data or methods are available upon reasonable request.

RESULTS

1.1 Conditional deletion of the PTH1R in the VSM lineage increases aortic fibrosis and VSM collagen gene expression.

Transgenic expression of a ligand-independent, constitutively active variant of the PTH1R -- PTH1R(H223R) hence caPTH1R -- suppressed aortic calcification, fibrosis and stiffness when expressed in VSM of LDLR−/− mice fed high fat diabetogenic diets (HFD)[10]. However, the role of endogenous PTH1R signaling tone in cardiovascular sclerosis remained unknown. To better understand the role of VSM PTH1R actions in arteriosclerosis, we generated SM22-Cre;PTH1R(fl/fl);LDLR−/− mice, using the SM22 promoter as a delivery module for VSM Cre-mediated PTH1R excision[19] in the VSM lineage[20]. Confocal immunofluorescence confirmed post-natal expression of endogenous PTH1R protein in VSM of murine aortas and coronary arteries, with little expression in myocardium (Figure 1A, 1B). PTH1R expression in arterial VSM overlapped that of lineage markers smooth muscle cell alpha actin (Acta2) (Figure 1C; segmental renal artery, and data not shown), and calponin (**Cnn1**; Figure 1D**;** aorta). Acta2 was not expressed in PTH1R-expressing kidney tubules (Figure 1C). PTH1R and Cnn1 also colocalized in the fibrofatty aortic adventitia (Figure 1D), indicating expression in microvascular pericytes of the VSM lineage[26]. PTH1R expression was also detected in the medial layer of human artery (Online Figure I). Immunofluorescence confirmed reduction of arterial PTH1R protein in SM22-Cre:PTH1R(fl/fl);LDLR−/− mice (Figure 1E). As first observed in male LDLR−/− mice, male SM22-Cre:PTH1R(fl/fl);LDLR−/− (PTH1R-VKO) and sibling PTH1R(fl/fl);LDLR−/− Cre-negative controls (CON) develop concomitant hyperglycemia and hyperlipidemia when fed HFD[1] (Online Figures II–III). Hypercholesterolemia was slightly reduced while hyperglycemia was slightly increased in PTH1R-VKO mice vs. CON siblings (Online Figure II). However, aortas from PTH1R-VKO mice accumulate significantly increased fibrillar collagen protein as assessed by Sircol assay[10, 27] (Figure 2A). Immunofluorescence for type I and type III collagens identified accumulation in intimal, medial, and adventitial compartments of both genotypes (Figure 2B, Online Figure IV). Aortic sinus atheroma, aortic calcification, and aortic stiffness were not increased with VSM PTH1R deficiency (Online Figures IV–V); thus, increased arterial fibrosis in PTH1R-VKO mice was uncoupled from calcification.

Primary VSM cultures were prepared from PTH1R-VKO mice and Cre-negative CON mice for in vitro mechanistic studies. Western blot analysis of VSM protein extracts confirmed reductions in PTH1R protein in PTH1R-VKO cultures (Figure 2C). Actions of PTH1R to restrict collagen production were demonstrated to be VSM cell-autonomous, deploying multiple methods to quantify fibrillar collagen expression. Primary cultures of VSM from PTH1R-VKO mice also exhibited more fibrillar collagen protein (viz., type I and type III on mass spectrometry and western blot), hydroxyproline content following acid hydrolysis, and associated collagen gene expression (*Col1a1*, *Col1a2*, *Col3a1*; Figures 2D, 2E, 2F, 2G, 2H).

Conversely, two genes associated with the early mineralizing phenotype, alkaline phosphatase (*TNAP*)[28] and *Col14a1*[29], were down-regulated in PTH1R-VKO (Figure 2H), even though transcription factors associated with inflammatory VSM mineralization were increased (*TNF*, *Msx2*, *Runx2*[1]). Uncoupling of fibrosis and mineralization was confirmed in culture, since PTH1R-VKO cells were deficient in TNAP activity and mineralized nodule formation (Online Figure VI). Acute downregulation of *PTH1R* by siRNA also upregulated *Col1a1*, *Col1a2*, and *Col3a1* (synthetic) gene expression in VSM, with concomitant reduction of the mature (contractile) phenotypic markers *Myh11*[30, 31] (Figure 2I), *Mylk/myosin light chain kinase* and *Cnn1/calponin* (Online Figure VII). Thus, endogenous PTH1R expression in the VSM lineage mitigates vascular fibrosis arising in LDLR−/− mice fed diabetogenic HFD, mediated via cell-autonomous inhibition of type I and type III collagen gene expression.

1.2 Nuclear extracts from PTH1R-VKO VSM accumulate higher levels of Mkl1, a MADS-box factor transcriptional co-activator.

To better understand the molecular mechanisms whereby PTH1R deficiency enhances the cell-autonomous synthetic phenotype of VSM, we analyzed nuclear protein –enriched extracts from PTH1R-VKO and CON VSM cultures by mass spectrometry, focusing upon transcription factors implicating in myofibroblast gene regulation. Ingenuity Pathway Analysis[32] (IPA) of proteins differentially activated with VSM PTH1R deficiency resembled that of profibrotic TGFb1 activation (Online Figure VIII**;** activation Z score = +6.031, F-test p(overlap) = 3.12E-9, and 1.36E-6 with Benjamini-Hochberg correction[33]), even though TGFb1 itself was not altered. Transcriptional regulators previously shown to participate in fibrosis, including Mkl1/Mrtfa, Fli1, Runx2, and Gata6, were significantly altered in PTH1R-VKO VSM (Online Figure VIII **and** Online Table I). Label-free quantitation of protein abundance by LC-MS/MS indicated significant upregulation of Mkl1/Mrtfa – a transactivating co-adaptor for the Srf/Mef family of MADS-box binding proteins[23] – in PTH1R-VKO cultures (Figure 3A). Fhl2, an integrin-regulated transcriptional co-adapter that can stabilize Mkl1[23], was also significantly increased (Figure 3A). Intriguingly, Fli1 and Gata6 – the latter an important regulator of the contractile VSM phenotype[30, 31, 34] -- were down-regulated with PTH1R deficiency (Figure 3A). Changes were confirmed by Western blot (Figure 3B, Online Figure IX, and data not shown). Mkl1 staining was detected in nuclear and cytoplasmic domains of arterial VSM and atheroma of LDLR−/− mice on HFD (Online Figure X). To characterize the potential functional consequences, we systematically deployed RNAi targeting nuclear proteins altered by PTH1R deficiency, assessing *Col1a1* and *Col3a1* expression. Targeting *Fhl2* had no impact on *Col1a1* and *Col3a1* upregulation observed with PTH1R deficiency (Online Figure XI), and *Fli1* siRNA had little impact (not shown). However, siRNA targeting Mkl1 significantly inhibited upregulation of *Col1a1* and *Col3a1* genes arising from VSM PTH1R deficiency (Figure 3C). Western blot analyses confirmed reductions in Mkl1 protein with siRNA targeting *Mkl1* (Figure 3B). Mkl1 siRNA had no impact on *Srf* or *Mef2d* (Figure 3D). Of note, knockdown of Mkl1 increased *Myh11* gene expression in CON cells, but was inactive in PTH1R-VKO VSM where *Myh11* expression was greatly reduced (Figure 3D). LC-MS/MS analysis of extracts from PTH1R-VKO VSM confirmed that the elevated Col1a1 and Col3a1 protein levels were reduced by siRNA targeting *Mkl1* (Figure 3E). Likewise, treatment of cells with the Mkl1 inhibitor

CCG1423[35] also mitigated upregulation of collagen gene expression (Figure 3F). Furthermore, KD025[36], an inhibitor of Rock2 kinase activity upstream of Mkl1[37], also reversed *Col3a1* upregulation in PTH1R-VKO VSM (Online Figure XII). Thus, PTH1R deficiency upregulates Mkl1 transcriptional programs involved in VSM fibrillar collagen matrix biosynthesis.

1.3 Col3a1 inhibition by PTH1R and activation by Mkl1 maps to a proximal promoter region encompassing a hybrid CT(A/T)$_6$GG MADS-box transcription factor element.

Type III collagen, a homotrimer encoded by the *Col3a1* gene, plays a vital role in aortic matrix physiology and strength, with *Col3a1* deficiency increasing aortic aneurysm (Ehlers-Danlos Syndrome Type IV[38]). Surprisingly few studies have examined the *Col3a1* promoter as relevant to tissue fibrogenesis[39, 40]. Analysis (ALGGEN[41]) of the mouse and human *Col3a1* promoters identified a conserved 64 bp element at nucleotides −82 to −19 relative to the transcription start site[40], encompassing a CT(A/T)$_6$GG motif at −22 to −31 (Figure 4A). This motif is a hybrid Mef2/Srf MADS-box cognate[42], and therefore a potential target of Mkl1-dependent transactivation and PTH1R-dependent inhibition. To better understand *Col3a1* transcription, we cloned the 3 kB mouse *Col3a1* promoter upstream of the luciferase (LUC) reporter gene, and examined its regulation by PTH1R and Mkl1. For these studies, we deployed the rat aortic VSM line A7r5, a cellular background that faithfully recapitulates key features of VSM gene transcription[43], with confirmation of key findings in primary mouse and human aortic VSM. As shown in Figure 4B, the 3 kb Col3a1 promoter is active and suppressed by co-expression of the constitutively active PTH1R caPTH1R[10, 44]. 5'-prime deletion analysis mapped regulation to the proximal 0.5 kb of the Col3a1 promoter (Figure 4B). A dinucleotide mutation of the CT(A/T)$_6$***GG*** motif to CT(A/T)$_6$***TT*** **(TTmut3')** reduced the basal activity of the 3kb *Col3a1* promoter, and abrogated suppression by caPTH1R. Similar results were observed in primary human aortic VSM and A7r5 rat aortic VSM (Figure 4B). Moreover, *Col3a1* promoter activity was increased in transfected primary mouse aortic VSM from PTH1R-deficient mice, dependent upon the intact hybrid motif (Online Figure XIII). Almost identical results were obtained when a dinucleotide mutation was introduced into the 5'region of this element (TTmut5'; Figure 4A, Online Figure XIII). Similar promoter responses were observed in HEK293T cells (Online Figure XIV).

Mkl1 is a co-adapter for the SRF/MEF2 family of DNA binding proteins[23]. Like Mkl1, siRNA targeting *Srf* also reduced *Col3a1* upregulation in response to PTH1R deficiency (Online Figure XV). Co-expression of Srf confirmed that *Col3a1* promoter was controlled by this MADS-box factor and required the intact CT(A/T)$_6$***GG*** motif (Figure 4C), further establishing the functionality of this conserved element. Mkl1 co-expression upregulated *Col3a1* promoter activity -- again dependent upon the intact CT(A/T)$_6$***GG*** cognate at –31 to –22 (Figure 4D, **see** Figure 4A) and inhibited by caPTH1R (Figure 4E). KD025 also inhibited Mkl1 activation of the *Col3a1* promoter (Figure 4F) as predicted (Online Figure XII). Chromatin immunoprecipitation (ChIP) assays demonstrated significantly increased Mkl1 protein associated with chromatin at *Col3a1* and *Col1a1* transcriptional start sites in PTH1R-VKO primary VSM cultures – but with no change in the background signal at the *TNF* promoter (Figure 4G, negative control). Similarly, analysis[41] of the mouse *Col1a1* gene identified a CT(A/T)$_6$***GG*** cognate 12.5 kbp upstream of the transcription initiation site. This

Col1a1 element conveyed activation by Mkl1 onto an unresponsive heterologous RSV promoter, was inhibited by caPTH1R, and dependent upon the intact CT(A/T)$_6$***GG*** motif (Online Figure XVI). ChIP assay identified increased Mkl1 coactivator binding to this region in the *Col1a1* promoter with VSM PTH1R deficiency (Online Figure XVI), as observed at the *Col1a1* transcriptional initiation site (Figure 4G). Regulation of collagen promoter activity by Mkl1 in A7r5 VSM cells appears to be overlapping with, but distinct from, phosphoregulatory events in the RPEL1[45] and SAP - leucine zipper linker domains that control Mkl1 nuclear accumulation. Phosphomimetic amino acid substitutions shown to increase[45] (PPLKSP PPLKAP) or decrease[46] (STPPVSP SEPPVEP) nuclear Mkl1 accumulation both reduced *Col3a1* promoter activity to an extent equivalent to that with PTH1R-mediated inhibition (Online Figure XVII). Thus, PTH1R- and Mkl1-dependent transcriptional regulation of *Col3a1* maps to a phylogenetically conserved proximal promoter element encompassing a functional hybrid[42] MADS-box cognate. A similar, functional cognate is present in the *Col1a1* promoter.

1.4 VSM lineage PTH1R deficiency increases C1r and C1s proteins in circulating plasma matrix vesicles.

We deployed DAVID[47] to the analysis of proteomic results of proteins in plasma membrane fractions prepared from PTH1R-VKO vs. CON cells (n=3 / genotype, 10 ug protein analyzed per sample). We utilized a cutoff of $p < 0.01$ for differences in protein abundance by LC-MS/MS between genotypes prior to analysis with DAVID. Of the 859 proteins meeting this threshold (Online Table II), 846 had DAVID IDs, with 302 of these (35.7%) with Gene Ontology Cell Component (GOTERM_CC) term of “Extracellular Exosome” (Benjamini-Hochberg / B-H corrected[33] p value = 1.7E-61, 2.7-fold enrichment). Indeed, a plot of GOTERM_CC vs. $-\log_{10}$(B-H corrected P value) revealed that proteins with this annotation were the most significantly altered (Figure 5A). Exosomes are members of the family of extracellular vesicles (EVs), with sizes that range between 50 nm and 500 nm in diameter. EVs in the 30 nm to 500 nm size range and elaborated by VSM play critical roles in arterial matrix biology[48]. We hypothesized that circulating plasma EVs from SM22-Cre;PTH1R(fl/fl);LDLR−/− mice might reflect the molecular signatures of arteriosclerotic VSM biology. Circulating plasma EV were prepared by differential centrifugation from SM22-Cre;PTH1R(fl/fl);LDLR−/− mice and PTH1R(fl/fl);LDLR−/− sibling controls on HFD (n = 5 males of each genotype). We then implemented Nanosight NS300 nanoparticle tracking[49] to characterize and quantify these circulating EVs. Inspection revealed 2 populations with peaks centered at ca. 60 nm and 150 nm in addition to likely protein aggregates < 30 nM (Online Figure XVIII). Enumeration revealed a 34% increase in circulating EVs in the 80 nm to 300 nm size range (Figure 5B**; n = 5/genotype**), and a non-significant trend within the 30 nm- to 80 nm range (Online Figure XIX). The bioactivity of these EVs differs between PTH1R-VKO and CON mice. While not regulating *Col3a1* or *Myh11* gene expression, EVs induced *TNAP* and *Osterix* expression in VSM (Online Figure XX). Activity was significantly reduced in circulating EVs isolated from PTH1R-VKO mice (Online Figure XX), paralleling mineralization defects of primary VSM cultures from PTH1R-VKO mice (Online Figure VI).

To better understand how VSM PTH1R deficiency impacts circulating EV composition, 10 micrograms of EV protein from each animal (n=3 / genotype) was partially resolved by SDS-PAGE, then characterized by LC-MS/MS complex mixture analysis[50]. Using LC-MS/MS label-free quantitation of protein abundance, and an initial p-value < 0.05 for cutoff, a total of 82 proteins were identified as significantly altered in PTH1R-VKO EVs vs CON EVs (Online Table III). Inspection rapidly identified the presence of complement proteins, confirmed by DAVID analysis[47] wherein 17 (21.2%) of these mapped to KEGG annotation for "Complement and Coagulation Cascades" (Online Figure XXI**;** B-H corrected p = 8.1E-21, 41 fold enrichment). Significant increases in C1r and C1s proteins in EVs from PTH1R-VKO mice (Figure 5C**;** C1ra and C1s1 in mouse) were of particular interest, since mutations in these proteins result in Ehlers-Danlos connective tissue syndromes (EDS) via unknown mechanisms[25]. As with EDS-associated *COL3A1* mutations[38], families with *C1R* EDS mutations are at risk for arterial dissection[24, 25].

Because C1ra was increased in circulating EV populations in PTH1R-VKO mice, we examined protein and mRNA expression data from PTH1R-VKO and CON VSM cultures. Label-free quantitation of plasma membrane protein abundances by LC-MS/MS further confirmed increases in VSM C1ra with PTH1R deficiency (Figure 5D), paralleling increases in VSM fibrillar collagens (Figure 2). VDAC1 (voltage-dependent anion-selective channel), a housekeeping membrane protein[51], was unaffected. Deploying a commercially available ELISA for mouse C1ra, we determined that C1ra accumulation in serum-free conditioned media was increased in PTH1R-VKO cultures vs. CON, and profoundly reduced by the Mkl1 inhibitor CCG1423 (Figure 5E). *C1ra* gene expression was significantly increased in PTH1R-VKO VSM (Figure 5F). The Mkl1 inhibitor CCG1423 almost completely reversed *C1ra* upregulation with VSM PTH1R deficiency (Figure 5F), as did treatment with KD025 (Online Figure XXII)[52]. Inspection of the mouse C1ra promoter revealed a MADS-box cognate at −1926 to −1916 relative to the transcriptional start site[53]. The 3kb mouse *C1ra* promoter is also activated by Mkl1 and inhibited by PTH1R receptor signaling (Figure 5G), paralleling *Col3a1* transcriptional responses above (Figure 4). Mkl1 activation of the *C1ra* promoter was inhibited by CCG1423 (Figure 5H) and KD025 (Online Figure XXIII). Thus, changes in the inhibitory PTH1R / Mkl1 signaling relay that control aortic VSM –mediated fibrosis and collagen gene expression also control VSM C1ra protein expression, reflected in circulating EV protein composition (Figure 6).

DISCUSSION

Vascular fibrosis is a feature of diabetes and other inflammatory diseases, a result of the synthetic activities of arterial VSM cells and myofibroblasts[2, 3, 30]. Hyperlipidemia and uremia, with or without diabetes, induce states of skeletal resistance to PTH1R signaling, with untoward actions on bone health[18, 54]. However, the impact of *vascular* PTH1R resistance and its consequence to cardiovascular health have not been examined, largely due to the lack of biomarkers that demarcate normal vascular PTH1R signaling tone. Of note, pharmacologic and genetic augmentation of VSM PTH1R signaling in the LDLR−/− mouse model of diet-induced dyslipidemia and diabetes reduces arteriosclerotic VSM actions[10]. We now extend these earlier results[10] to show that endogenous VSM PTH1R signaling limits VSM collagen production, mediated via the cell-autonomous inhibition of Mkl1-dependent

transcriptional activation. This has therapeutic implications. Rock2 kinase functions upstream of Mkl1 and Stat3 activation, and is being targeted in several clinically relevant settings including idiopathic pulmonary fibrosis [52] and graft-vs-host disease[55], and the inhibitor KD025 has had favorable outcomes in chronic graft-vs-host disease[55]. Our data indicate that the arterial fibrosis programs in the HFD-induced LDLR−/− mouse model significantly worsen in the absence of VSM PTH1R signaling and proceed via Mkl1. Thus, KD025 treatment may prove useful in the treatment of vascular fibrosis[56]. The unmet cardiovascular management needs of patients afflicted with chronic kidney disease (CKD) and concomitant resistance to PTH1R signaling are amongst the most salient[57]. CKD induces PTH1R resistance in part due to renally-cleared PTH metabolites that inhibit PTH1R activation[57,58]. Future experimentation will address whether KD025 could be repurposed to mitigate arteriosclerosis in CKD with or without diabetes. Moreover, since our data indicate that VSM lineage – dependent vascular fibrosls can be uncoupled from the extent of aortic calcification and atheroma formation, each feature of the arteriosclerotic phenotype must be assessed with therapeutic intervention.

Another novel and clinically-relevant result was that circulating EVs contain biomarkers reflecting VSM PTH1R activity. Currently, we have no molecular biomarker or physiological metric that demarcates a healthy set-point for vascular PTH1R signaling. Circulating EVs have emerged as “liquid biopsies” that contain cell-specific metabolic information in addition to important endocrine/paracrine regulatory cues[59]. We have identified C1r as one novel VSM target of PTH1R and Mkl1 regulation – studies first prompted from analyses of *circulating* EVs from PTH1R-VKO mice. The presence of C1r in circulating EVs caught our attention because mutations in C1r drive Type VIII Ehlers-Danlos Syndrome (EDS). EDS is characterized a spectrum of mutations causing skin, skeletal, and vascular abnormalities arising from abnormal collagenous tissue metabolism[24, 25, 38]. The mechanism of *C1r*-associated EDS Type VIII is unknown, but 15% of patients exhibit aortic and cerebrovascular aneurysm or dissection[24, 25]. This is reminiscent of EDS Type IV arising from *Col3a1* mutations; aortic rupture is responsible for >60% of deaths in afflicted families[38]. The role if any for C1r in arteriosclerosis is unknown. Nevertheless, the identification of C1r as a circulating EV constituent -- entrained to the same VSM PTH1/Mkl1 regulatory relay as Col3a1 -- reveals that EV C1r serves as one index of fibrotic VSM activity. As such, EVs could help guide dose-ranging studies during treatment for arteriosclerosis. C1r or a similar EV biomarker could also help establish the healthy VSM set-point for PTH1R signaling. Our studies demonstrating reduced *TNAP* induction by circulating EVs from PTH1R-VKO mice provide further support for this notion. Arterial VSM PTH1R signaling undergoes tachyphylaxis, with prior exposure down-regulating subsequent PTH1R responses[14]. Sustained elevations in PTH -- as occurs with primary hyperparathyroidism or CKD -- are predicted to induce arterial PTH1R resistance[14], but to date we have no index of vascular PTH1R signaling tone. Interestingly, in mild primary hyperparathyroidism, serum PTH levels track long-term cardiovascular mortality risk[60]. Future experiments will determine if hyperparathyroidism upregulates Mkl1, stimulates arterial collagen and C1r production, and increases circulating EV C1r levels as a reflection of compromised VSM PTH1R actions.

Hybrid SRF/MEF2 CT(A/T)$_6$GG CArG elements were discovered as a dual-specificity binding cognate encoded within the *MyoD* distal regulatory region (DRR) enhancer[42]. The DRR is central to postnatal expression of *MyoD* in skeletal muscle[61] arising from satellite cells during regeneration[42]. As satellite cells mature to proliferative then post-proliferative myoblasts and differentiated myotubes, MyoD expression driven by the DRR switches from SRF-dependence to MEF2-dependence[42]. Approximately 200,000 hybrid cognates are predicted to exist in the mammalian genome, and have yet to be systematically characterized or widely recognized. Whether cell maturation-specific regulation [42] holds for all of these cognates -- or the functional cognates we newly identify -- remains to be examined. A prototypic CC(A/T)$_6$GG CArG element identified in the proximal *Col1a2* promoter is activated in cardiac fibroblasts with myocardial infarction[62]. Myocardial fibroblasts and adipose pericytes may also be held in check by PTH1R signals but this remains to be determined.

While gain-of-function VSM PTH1R signaling reduces *both* vascular fibrosis and calcification[10], VSM PTH1R deficiency increased vascular fibrosis *without* increasing vascular calcification. This was independent of atheroma size. The reasons for the uncoupling of vascular fibrosis and calcification with VSM PTH1R deficiency have yet to be determined, but likely relate to impaired VSM expression of *TNAP* (Figure 2I). *TNAP* encodes an enzyme vital to osteogenic mineralization in skeletal and vascular venues[28] Intriguingly, deficiency in osteogenic signaling was also evident in the bioactivity of circulating EVs from PTH1R-VKO mice (Online Figure XX). Because paracrine signals are important activators of osteogenic mineralization[22], an in-depth study of the PTH1R-regulated VSM secretome -- including Wnt modulators associated with EVs[48] -- promises to be enlightening. Indeed, circulating EVs suppress VSM *Axin2*, a target and inhibitor of Wnt signaling (Online Figure XX). However, origins of circulating EVs altered by VSM PTH1R deficiency remain to determined. The SM22-Cre transgene is expressed broadly in the VSM lineage -- including pericytic adipocyte progenitors[26] -- and bidirectional paracrine EV cross-talk occurs between the endothelium and adjacent mesenchyme in adipose[49]. This may be relevant to fibrosis involving the adventitial-medial junction as well as the intima and media (Figure S4, and ref. [10]).

Our data point to arterial calcification[10, 22, 63] as a key determinant of aortic stiffness in the LDLR−/− mouse model[1]. The osteogenic phenotype of mesenchymal cells is favored on matrices with stiffness of 25 – 40 kPa[64] (below the optimal fibrogenic stiffness of > 100 kPa[64]). Thus, aberrant mechanosensation[65] in PTH1R-VKO mice may uncouple fibrogenesis and mineralization. However, reciprocal changes in synthetic (collagens) and contractile (*Myh11*, *Mylk, Cnn1*) programs[30, 31] with reduced osteogenic calcification highlight a broader impact on the VSM phenotype. Dysregulated SRF/Mkl1 signaling itself inhibits cell-type-specific gene expression that defines differentiation[66]. Chronically increased Mkl1 activity is predicted to inhibit *both* myogenic and osteogenic potential with VSM phenotypic modulation, and normal VSM PTH1R signaling supports cell-type-specific terminal differentiation (e.g., *Myh11*, Figures 2I, 3D) while limiting fibrosis. PTH1R-dependent support of Gata6 will also be important[34].

There are limitations to our study. While we discover a novel VSM cell-autonomous PTH1R – Mkl1 transcriptional relay that controls vascular fibrosis, the precise molecular mechanisms remain to be elucidated. Mkl1 is controlled by interactions with cytoplasmic and nuclear G-actin pools that determine Mkl1 nuclear export/import cycling and transactivation[23]. The observation that CCG1423[35] and Mkl1 phosphomimetic mutations within RPEL1 and SAP-leucine zipper linker domains phenocopy caPTH1R actions suggest mechanisms are overlapping yet distinct from G-actin regulation[45, 46]. Future studies will emphasize Mkl1 protein-protein interactions and turnover as regulated by PTH1R activity. Because Wnt/beta-catenin relays are also important in regulating VSM *Col1a1*[10] and *Col3a1* (Online Figure XXIV and [10]), beta-catenin interactions with Mkl1 complexes will be examined. Nevertheless, our data demonstrate that endogenous PTH1R signaling restricts arterial collagen production by the VSM lineage, mediated in part via a novel Mkl1 transcriptional relay that controls type III and type I collagen gene expression and reflected in circulating EV biochemistry. As such, this pathway affords new strategies to maintain and monitor homeostatic VSM PTH1R/Mkl1 signaling as a therapeutic approach to mitigate vascular fibrosis.

Supplementary Material

Refer to Web version on PubMed Central for supplementary material.

Acknowledgments

SOURCES OF FUNDING

Supported by NIH Grants HL114806, HL069229, and DK011794, by

American Diabetes Association grant #1-18-IBS-224, the JD and Maggie E Wilson Endowed Chair, and the Louis V. Avioli Professorship.

Nonstandard Abbreviations and Acronyms:

A7r5	vascular smooth muscle cell line derived from thoracic aorta of embryonic rats
B-H	Benjamini-Hochberg correction for false discovery rate
C1ra	complement component 1, r subcomponent A
C1s1	complement component 1, s subcomponent 1
CArG box	C-A/T rich –G DNA binding motif $CC(A/T)_6GG$, $CT(A/T)_6GG$
CCG1423	Mkl1/Srf inhibitor
ChIP	chromatin immunoprecipitation
CKD-MBD	chronic kidney disease – mineral and bone disorder
CMV	cytomegalovirus promoter/enhancer vector

Col1a1	type I alpha(1) collagen
Col3a1	type III alpha(1) collagen
Col14a1	type XIV alpha(1) collagen
CON	control mice, viz., PTH1R(fl/fl);LDLR−/− mice
Cre	causes recombination, bacteriophage P1 recombinase
DAPI	4′,6-diamidino-2-phenylindole
DAVID	Database for Annotation, Visualization and Integrated Discovery
EDS	Ehlers-Danlos Syndrome
EVs	extracellular microvesicles in the 30 to 500 nm diameter range
Fhl2	four and a half LIM domains 2fh2
G-actin	globular actin
HFD	high fat diet, Harland TD.88137 Western diet
IPA	Ingenuity Pathway Analysis
KD025	a Rock2 kinase family inhibitor
LC-MS/MS	liquid chromatography – tandem mass spectrometry
LDLR	low density lipoprotein receptor
LUC	luciferase reporter
MADS	MCM1, Agamous, Deficiens, and Srf DNA binding domain
MEF2	myocyte enhancer factor 2
Mkl1	megakaryoblastic leukemia (translocation) 1, a.k.a. Mrtfa
Mrtfa	myocardin related transcription factor -A, a.k.a. Mkl1
Myh11	smooth muscle specific myosin heavy chain 11
Mylk	myosin light chain kinase
Msx2	muscle segment homeobox 2
Osx	osteoblast transcription factor osterix, a.k.a. Sp7
PPARG	peroxisome proliferator activated receptor gamma
PTH	parathyroid hormone

PTH1R	PTH/PTHrP receptor
PTHrP	parathyroid hormone related polypeptide
PTH1R(fl/fl)	PTH1R gene floxed, e.g. flanked by lox P
PTHR1-VKO	PTH1R VSM conditional knockout on LDLR−/− background; SM22-Cre;PTH1R(fl/fl);LDLR−/−
RNAi	RNA interference
Rock2	Rho associated coiled-coil containing protein kinase 2
RPEL domain	Arg-Pro-Glu-Leu repeat domain that binds globular actin
RSV	Rous Sarcoma Virus
Runx2	Runt-related transcription factor 2
SAP domain, SAF-A/B	Acinus, and PIAS domain
SDS-PAGE	sodium dodecyl sulfate – polyacrylamide gel electrophoresis
siRNA	small interfering RNA
SM22-Cre	transgene expressing bacterial Cre recombinase from SM22 (transgelin) promoter
Srf	serum response factor
TBS	Tris-buffered saline
TNAP	bone-liver-kidney alkaline phosphatase a.k.a. tissue non-specific alkaline phosphatase
TNF	tumor necrosis factor
VDAC	Voltage-dependent anion-selective channel
VKO	VSM knockout
VSM	vascular smooth muscle lineage

REFERENCES

1. Stabley JN and Towler DA. Arterial Calcification in Diabetes Mellitus: Preclinical Models and Translational Implications. Arterioscler Thromb Vasc Biol. 2017;37:205–217. [PubMed: 28062508]
2. Lan TH, Huang XQ and Tan HM. Vascular fibrosis in atherosclerosis. Cardiovasc Pathol. 2013;22:401–7. [PubMed: 23375582]
3. Greenwald SE. Ageing of the conduit arteries. J Pathol. 2007;211:157–72. [PubMed: 17200940]
4. Grundy SM. Metabolic syndrome pandemic. Arterioscler Thromb Vasc Biol. 2008;28:629–36. [PubMed: 18174459]
5. Bostrom KI. Where do we stand on vascular calcification? Vascul Pharmacol. 2016;84:8–14. [PubMed: 27260939]

6. Goettsch C, Kjolby M and Aikawa E. Sortilin and Its Multiple Roles in Cardiovascular and Metabolic Diseases. Arterioscler Thromb Vasc Biol. 2018;38:19–25. [PubMed: 29191923]
7. Raaz U, Schellinger IN, Chernogubova E, Warnecke C, Kayama Y, Penov K, Hennigs JK, Salomons F, Eken S, Emrich FC, Zheng WH, Adam M, Jagger A, Nakagami F, Toh R, Toyama K, Deng A, Buerke M, Maegdefessel L, Hasenfuss G, Spin JM and Tsao PS. Transcription Factor Runx2 Promotes Aortic Fibrosis and Stiffness in Type 2 Diabetes Mellitus. Circ Res. 2015;117:513–24. [PubMed: 26208651]
8. Heath JM, Sun Y, Yuan K, Bradley WE, Litovsky S, Dell'Italia LJ, Chatham JC, Wu H and Chen Y. Activation of AKT by O-linked N-acetylglucosamine induces vascular calcification in diabetes mellitus. Circ Res. 2014;114:1094–102. [PubMed: 24526702]
9. Pescatore LA, Gamarra LF and Liberman M. Multifaceted Mechanisms of Vascular Calcification in Aging. Arterioscler Thromb Vasc Biol. 2019;39:1307–1316. [PubMed: 31144990]
10. Cheng SL, Shao JS, Halstead LR, Distelhorst K, Sierra O and Towler DA. Activation of vascular smooth muscle parathyroid hormone receptor inhibits Wnt/beta-catenin signaling and aortic fibrosis in diabetic arteriosclerosis. Circ Res. 2010;107:271–82. [PubMed: 20489161]
11. Lanske B and Kronenberg HM. Parathyroid hormone-related peptide (PTHrP) and parathyroid hormone (PTH)/PTHrP receptor. Crit Rev Eukaryot Gene Expr. 1998;8:297–320. [PubMed: 9807698]
12. Qian J, Colbert MC, Witte D, Kuan CY, Gruenstein E, Osinska H, Lanske B, Kronenberg HM and Clemens TL. Midgestational lethality in mice lacking the parathyroid hormone (PTH)/PTH-related peptide receptor is associated with abrupt cardiomyocyte death. Endocrinology. 2003;144:1053–61. [PubMed: 12586782]
13. Gray C, Bratt D, Lees J, daCosta M, Plant K, Watson OJ, Solaymani-Kohal S, Tazzyman S, Serbanovic-Canic J, Crossman DC, Keavney BD, Haase A, McMahon K, Gering M, Roehl H, Evans PC and Chico TJ. Loss of function of parathyroid hormone receptor 1 induces Notch-dependent aortic defects during zebrafish vascular development. Arterioscler Thromb Vasc Biol. 2013;33:1257–63. [PubMed: 23559631]
14. Nyby MD, Hino T, Berger ME, Ormsby BL, Golub MS and Brickman AS. Desensitization of vascular tissue to parathyroid hormone and parathyroid hormone-related protein. Endocrinology. 1995;136:2497–504. [PubMed: 7750471]
15. Yu N, Donnan PT, Flynn RW, Murphy MJ, Smith D, Rudman A and Leese GP. Increased mortality and morbidity in mild primary hyperparathyroid patients. The Parathyroid Epidemiology and Audit Research Study (PEARS). Clin Endocrinol (Oxf). 2010;73:30–4. [PubMed: 20039887]
16. Osto E, Fallo F, Pelizzo MR, Maddalozzo A, Sorgato N, Corbetti F, Montisci R, Famoso G, Bellu R, Luscher TF, Iliceto S and Tona F. Coronary microvascular dysfunction induced by primary hyperparathyroidism is restored after parathyroidectomy. Circulation. 2012;126:1031–9. [PubMed: 22821942]
17. Kosch M, Hausberg M, Vormbrock K, Kisters K, Gabriels G, Rahn KH and Barenbrock M. Impaired flow-mediated vasodilation of the brachial artery in patients with primary hyperparathyroidism improves after parathyroidectomy. Cardiovasc Res. 2000;47:813–8. [PubMed: 10974230]
18. Thompson B and Towler DA. Arterial calcification and bone physiology: role of the bone-vascular axis. Nat Rev Endocrinol. 2012;8:529–43. [PubMed: 22473330]
19. Kobayashi T, Chung UI, Schipani E, Starbuck M, Karsenty G, Katagiri T, Goad DL, Lanske B and Kronenberg HM. PTHrP and Indian hedgehog control differentiation of growth plate chondrocytes at multiple steps. Development. 2002;129:2977–86. [PubMed: 12050144]
20. Holtwick R, Gotthardt M, Skryabin B, Steinmetz M, Potthast R, Zetsche B, Hammer RE, Herz J and Kuhn M. Smooth muscle-selective deletion of guanylyl cyclase-A prevents the acute but not chronic effects of ANP on blood pressure. Proc Natl Acad Sci U S A. 2002;99:7142–7. [PubMed: 11997476]
21. Ishibashi S, Brown MS, Goldstein JL, Gerard RD, Hammer RE and Herz J. Hypercholesterolemia in low density lipoprotein receptor knockout mice and its reversal by adenovirus-mediated gene delivery. J Clin Invest. 1993;92:883–93. [PubMed: 8349823]

22. Cheng SL, Ramachandran B, Behrmann A, Shao JS, Mead M, Smith C, Krchma K, Bello Arredondo Y, Kovacs A, Kapoor K, Brill LM, Perera R, Williams BO and Towler DA. Vascular smooth muscle LRP6 limits arteriosclerotic calcification in diabetic LDLR−/− mice by restraining noncanonical Wnt signals. Circ Res. 2015;117:142–56. [PubMed: 26034040]

23. Sward K, Stenkula KG, Rippe C, Alajbegovic A, Gomez MF and Albinsson S. Emerging roles of the myocardin family of proteins in lipid and glucose metabolism. J Physiol. 2016;594:4741–52. [PubMed: 27060572]

24. D'Hondt S, Van Damme T and Malfait F. Vascular phenotypes in nonvascular subtypes of the Ehlers-Danlos syndrome: a systematic review. Genet Med. 2018;20:562–573. [PubMed: 28981071]

25. Kapferer-Seebacher I, Pepin M, Werner R, Aitman TJ, Nordgren A, Stoiber H, Thielens N, Gaboriaud C, Amberger A, Schossig A, Gruber R, Giunta C, Bamshad M, Bjorck E, Chen C, Chitayat D, Dorschner M, Schmitt-Egenolf M, Hale CJ, Hanna D, Hennies HC, Heiss-Kisielewsky I, Lindstrand A, Lundberg P, Mitchell AL, Nickerson DA, Reinstein E, Rohrbach M, Romani N, Schmuth M, Silver R, Taylan F, Vandersteen A, Vandrovcova J, Weerakkody R, Yang M, Pope FM, Molecular Basis of Periodontal EDSC, Byers PH and Zschocke J. Periodontal Ehlers-Danlos Syndrome Is Caused by Mutations in C1R and C1S, which Encode Subcomponents C1r and C1s of Complement. Am J Hum Genet. 2016;99:1005–1014. [PubMed: 27745832]

26. Traktuev DO, Merfeld-Clauss S, Li J, Kolonin M, Arap W, Pasqualini R, Johnstone BH and March KL. A population of multipotent CD34-positive adipose stromal cells share pericyte and mesenchymal surface markers, reside in a periendothelial location, and stabilize endothelial networks. Circ Res. 2008;102:77–85. [PubMed: 17967785]

27. Li YY, Feng Y, McTiernan CF, Pei W, Moravec CS, Wang P, Rosenblum W, Kormos RL and Feldman AM. Downregulation of matrix metalloproteinases and reduction in collagen damage in the failing human heart after support with left ventricular assist devices. Circulation. 2001;104:1147–52. [PubMed: 11535571]

28. Sheen CR, Kuss P, Narisawa S, Yadav MC, Nigro J, Wang W, Chhea TN, Sergienko EA, Kapoor K, Jackson MR, Hoylaerts MF, Pinkerton AB, O'Neill WC and Millan JL. Pathophysiological role of vascular smooth muscle alkaline phosphatase in medial artery calcification. J Bone Miner Res. 2015;30:824–36. [PubMed: 25428889]

29. Paic F, Igwe JC, Nori R, Kronenberg MS, Franceschetti T, Harrington P, Kuo L, Shin DG, Rowe DW, Harris SE and Kalajzic I. Identification of differentially expressed genes between osteoblasts and osteocytes. Bone. 2009;45:682–92. [PubMed: 19539797]

30. Basatemur GL, Jorgensen HF, Clarke MCH, Bennett MR and Mallat Z. Vascular smooth muscle cells in atherosclerosis. Nat Rev Cardiol. 2019.

31. Petsophonsakul P, Furmanik M, Forsythe R, Dweck M, Schurink GW, Natour E, Reutelingsperger C, Jacobs M, Mees B and Schurgers L. Role of Vascular Smooth Muscle Cell Phenotypic Switching and Calcification in Aortic Aneurysm Formation. Arterioscler Thromb Vasc Biol. 2019;39:1351–1368. [PubMed: 31144989]

32. Kramer A, Green J, Pollard J Jr. and Tugendreich S. Causal analysis approaches in Ingenuity Pathway Analysis. Bioinformatics. 2014;30:523–30. [PubMed: 24336805]

33. Benjamini Y and Hochberg Y. Controlling the False Discovery Fate: a Practical and Powerful Approach to Multiple Testing. J R Stastist Soc B. 1995;57:289–300.

34. Srivastava R, Rolyan H, Xie Y, Li N, Bhat N, Hong L, Esteghamat F, Adeniran A, Geirsson A, Zhang J, Ge G, Nobrega M, Martin KA and Mani A. TCF7L2 (Transcription Factor 7-Like 2) Regulation of GATA6 (GATA-Binding Protein 6)-Dependent and -Independent Vascular Smooth Muscle Cell Plasticity and Intimal Hyperplasia. Arterioscler Thromb Vasc Biol. 2019;39:250–262. [PubMed: 30567484]

35. Hayashi K, Watanabe B, Nakagawa Y, Minami S and Morita T. RPEL proteins are the molecular targets for CCG-1423, an inhibitor of Rho signaling. PLoS One. 2014;9:e89016. [PubMed: 24558465]

36. Weiss JM, Chen W, Nyuydzefe MS, Trzeciak A, Flynn R, Tonra JR, Marusic S, Blazar BR, Waksal SD and Zanin-Zhorov A. ROCK2 signaling is required to induce a subset of T follicular helper cells through opposing effects on STATs in autoimmune settings. Sci Signal. 2016;9:ra73. [PubMed: 27436361]

37. Htwe SS, Cha BH, Yue K, Khademhosseini A, Knox AJ and Ghaemmaghami AM. Role of Rho-Associated Coiled-Coil Forming Kinase Isoforms in Regulation of Stiffness-Induced Myofibroblast Differentiation in Lung Fibrosis. Am J Respir Cell Mol Biol. 2017;56:772–783. [PubMed: 28225294]
38. Kuivaniemi H and Tromp G. Type III collagen (COL3A1): Gene and protein structure, tissue distribution, and associated diseases. Gene. 2019;707:151–171. [PubMed: 31075413]
39. Jimenez SA, Gaidarova S, Saitta B, Sandorfi N, Herrich DJ, Rosenbloom JC, Kucich U, Abrams WR and Rosenbloom J. Role of protein kinase C-delta in the regulation of collagen gene expression in scleroderma fibroblasts. J Clin Invest. 2001;108:1395–403. [PubMed: 11696585]
40. Ruteshouser EC and de Crombrugghe B. Characterization of two distinct positive cis-acting elements in the mouse alpha 1 (III) collagen promoter. J Biol Chem. 1989;264:13740–4. [PubMed: 2760041]
41. Farre D, Roset R, Huerta M, Adsuara JE, Rosello L, Alba MM and Messeguer X. Identification of patterns in biological sequences at the ALGGEN server: PROMO and MALGEN. Nucleic Acids Res. 2003;31:3651–3. [PubMed: 12824386]
42. L'Honore A, Rana V, Arsic N, Franckhauser C, Lamb NJ and Fernandez A. Identification of a new hybrid serum response factor and myocyte enhancer factor 2-binding element in MyoD enhancer required for MyoD expression during myogenesis. Mol Biol Cell. 2007;18:1992–2001. [PubMed: 17377068]
43. Bidder M, Shao JS, Charlton-Kachigian N, Loewy AP, Semenkovich CF and Towler DA. Osteopontin transcription in aortic vascular smooth muscle cells is controlled by glucose-regulated upstream stimulatory factor and activator protein-1 activities. J Biol Chem. 2002;277:44485–96. [PubMed: 12200434]
44. Schipani E, Kruse K and Juppner H. A constitutively active mutant PTH-PTHrP receptor in Jansen-type metaphyseal chondrodysplasia. Science. 1995;268:98–100. [PubMed: 7701349]
45. Panayiotou R, Miralles F, Pawlowski R, Diring J, Flynn HR, Skehel M and Treisman R. Phosphorylation acts positively and negatively to regulate MRTF-A subcellular localisation and activity. Elife. 2016;5.
46. Muehlich S, Wang R, Lee SM, Lewis TC, Dai C and Prywes R. Serum-induced phosphorylation of the serum response factor coactivator MKL1 by the extracellular signal-regulated kinase 1/2 pathway inhibits its nuclear localization. Mol Cell Biol. 2008;28:6302–13. [PubMed: 18694962]
47. Huang da W, Sherman BT and Lempicki RA. Systematic and integrative analysis of large gene lists using DAVID bioinformatics resources. Nat Protoc. 2009;4:44–57. [PubMed: 19131956]
48. Kapustin AN, Chatrou ML, Drozdov I, Zheng Y, Davidson SM, Soong D, Furmanik M, Sanchis P, De Rosales RT, Alvarez-Hernandez D, Shroff R, Yin X, Muller K, Skepper JN, Mayr M, Reutelingsperger CP, Chester A, Bertazzo S, Schurgers LJ and Shanahan CM. Vascular smooth muscle cell calcification is mediated by regulated exosome secretion. Circ Res. 2015;116:1312–23. [PubMed: 25711438]
49. Crewe C, Joffin N, Rutkowski JM, Kim M, Zhang F, Towler DA, Gordillo R and Scherer PE. An Endothelial-to-Adipocyte Extracellular Vesicle Axis Governed by Metabolic State. Cell. 2018;175:695–708 e13. [PubMed: 30293865]
50. Ramachandran B, Stabley JN, Cheng SL, Behrmann AS, Gay A, Li L, Mead M, Kozlitina J, Lemoff A, Mirzaei H, Chen Z and Towler DA. A GTPase-activating protein-binding protein (G3BP1)/antiviral protein relay conveys arteriosclerotic Wnt signals in aortic smooth muscle cells. J Biol Chem. 2018;293:7942–7968. [PubMed: 29626090]
51. Sampson MJ, Lovell RS and Craigen WJ. The murine voltage-dependent anion channel gene family. Conserved structure and function. J Biol Chem. 1997;272:18966–73. [PubMed: 9228078]
52. Shimizu Y, Dobashi K, Sano T and Yamada M. ROCK activation in lung of idiopathic pulmonary fibrosis with oxidative stress. Int J Immunopathol Pharmacol. 2014;27:37–44. [PubMed: 24674677]
53. Byun SJ, Jeon IS, Lee H and Kim TY. IFN-gamma upregulates expression of the mouse complement C1rA gene in keratinocytes via IFN-regulatory factor-1. J Invest Dermatol. 2007;127:1187–96. [PubMed: 17159910]

54. Sage AP, Lu J, Atti E, Tetradis S, Ascenzi MG, Adams DJ, Demer LL and Tintut Y. Hyperlipidemia induces resistance to PTH bone anabolism in mice via oxidized lipids. J Bone Miner Res. 2011;26:1197–206. [PubMed: 21611962]
55. Flynn R, Paz K, Du J, Reichenbach DK, Taylor PA, Panoskaltsis-Mortari A, Vulic A, Luznik L, MacDonald KK, Hill GR, Nyuydzefe MS, Weiss JM, Chen W, Trzeciak A, Serody JS, Aguilar EG, Murphy WJ, Maillard I, Munn D, Koreth J, Cutler CS, Antin JH, Ritz J, Waksal SD, Zanin-Zhorov A and Blazar BR. Targeted Rho-associated kinase 2 inhibition suppresses murine and human chronic GVHD through a Stat3-dependent mechanism. Blood. 2016;127:2144–54. [PubMed: 26983850]
56. Massy Z and Drueke T. Adynamic bone disease is a predominant bone pattern in early stages of chronic kidney disease. J Nephrol. 2017;30:629–634. [PubMed: 28405928]
57. Hruska KA, Seifert M and Sugatani T. Pathophysiology of the chronic kidney disease-mineral bone disorder. Curr Opin Nephrol Hypertens. 2015;24:303–9. [PubMed: 26050115]
58. London GM, Marchais SJ, Guerin AP and de Vernejoul MC. Ankle-brachial index and bone turnover in patients on dialysis. J Am Soc Nephrol. 2015;26:476–83. [PubMed: 25231881]
59. Jansen F, Nickenig G and Werner N. Extracellular Vesicles in Cardiovascular Disease: Potential Applications in Diagnosis, Prognosis, and Epidemiology. Circ Res. 2017;120:1649–1657. [PubMed: 28495995]
60. Yu N, Leese GP and Donnan PT. What predicts adverse outcomes in untreated primary hyperparathyroidism? The Parathyroid Epidemiology and Audit Research Study (PEARS). Clin Endocrinol (Oxf). 2013;79:27–34. [PubMed: 23506565]
61. Chen JC, Ramachandran R and Goldhamer DJ. Essential and redundant functions of the MyoD distal regulatory region revealed by targeted mutagenesis. Dev Biol. 2002;245:213–23. [PubMed: 11969267]
62. Small EM, Thatcher JE, Sutherland LB, Kinoshita H, Gerard RD, Richardson JA, Dimaio JM, Sadek H, Kuwahara K and Olson EN. Myocardin-related transcription factor-a controls myofibroblast activation and fibrosis in response to myocardial infarction. Circ Res. 2010;107:294–304. [PubMed: 20558820]
63. Cheng SL, Behrmann A, Shao JS, Ramachandran B, Krchma K, Bello Arredondo Y, Kovacs A, Mead M, Maxson R and Towler DA. Targeted reduction of vascular Msx1 and Msx2 mitigates arteriosclerotic calcification and aortic stiffness in LDLR-deficient mice fed diabetogenic diets. Diabetes. 2014;63:4326–37. [PubMed: 25056439]
64. Engler AJ, Sen S, Sweeney HL and Discher DE. Matrix elasticity directs stem cell lineage specification. Cell. 2006;126:677–89. [PubMed: 16923388]
65. Humphrey JD, Schwartz MA, Tellides G and Milewicz DM. Role of mechanotransduction in vascular biology: focus on thoracic aortic aneurysms and dissections. Circ Res. 2015;116:1448–61. [PubMed: 25858068]
66. Ikeda T, Hikichi T, Miura H, Shibata H, Mitsunaga K, Yamada Y, Woltjen K, Miyamoto K, Hiratani I, Yamada Y, Hotta A, Yamamoto T, Okita K and Masui S. Srf destabilizes cellular identity by suppressing cell-type-specific gene expression programs. Nat Commun. 2018;9:1387. [PubMed: 29643333]
67. DeMarco VG, Habibi J, Jia G, Aroor AR, Ramirez-Perez FI, Martinez-Lemus LA, Bender SB, Garro M, Hayden MR, Sun Z, Meininger GA, Manrique C, Whaley-Connell A and Sowers JR. Low-Dose Mineralocorticoid Receptor Blockade Prevents Western Diet-Induced Arterial Stiffening in Female Mice. Hypertension. 2015;66:99–107. [PubMed: 26015449]
68. Reddy GK and Enwemeka CS. A simplified method for the analysis of hydroxyproline in biological tissues. Clin Biochem. 1996;29:225–9. [PubMed: 8740508]
69. Boudreaux JM and Towler DA. Synergistic induction of osteocalcin gene expression: identification of a bipartite element conferring fibroblast growth factor 2 and cyclic AMP responsiveness in the rat osteocalcin promoter. J Biol Chem. 1996;271:7508–15. [PubMed: 8631781]
70. Schindelin J, Arganda-Carreras I, Frise E, Kaynig V, Longair M, Pietzsch T, Preibisch S, Rueden C, Saalfeld S, Schmid B, Tinevez JY, White DJ, Hartenstein V, Eliceiri K, Tomancak P and Cardona A. Fiji: an open-source platform for biological-image analysis. Nat Methods. 2012;9:676–82. [PubMed: 22743772]

71. Lane RE, Korbie D, Anderson W, Vaidyanathan R and Trau M. Analysis of exosome purification methods using a model liposome system and tunable-resistive pulse sensing. Sci Rep. 2015;5:7639. [PubMed: 25559219]

72. Faul F, Erdfelder E, Lang AG and Buchner A. G*Power 3: a flexible statistical power analysis program for the social, behavioral, and biomedical sciences. Behav Res Methods. 2007;39:175–91. [PubMed: 17695343]

73. Wirka RC, Wagh D, Paik DT, Pjanic M, Nguyen T, Miller CL, Kundu R, Nagao M, Coller J, Koyano TK, Fong R, Woo YJ, Liu B, Montgomery SB, Wu JC, Zhu K, Chang R, Alamprese M, Tallquist MD, Kim JB and Quertermous T. Atheroprotective roles of smooth muscle cell phenotypic modulation and the TCF21 disease gene as revealed by single-cell analysis. Nat Med. 2019;25:1280–1289. [PubMed: 31359001]

NOVELTY AND SIGNIFICANCE

What Is Known?

- Dysmetabolic states such as hyperlipidemia, hyperparathyroidism, and type 2 diabetes with or without chronic kidney disease increase cardiovascular fibrosis, mediated in part via upregulation of osteofibrotic gene regulatory programs best characterized in the skeleton.
- The receptor for the prototypic bone anabolic hormones, parathyroid hormone (PTH) and PTH-related polypeptide, is expressed in arterial vascular smooth muscle. However, role of endogenous PTH1R activity in cardiovascular disease is poorly characterized.
- Signaling via the PTH/PTHrP receptor, a.k.a. PTH1R, is perturbed in hyperparathyroidism, hyperlipidemia, diabetes and chronic kidney disease – settings of increased cardiovascular morbidity and mortality.

What New Information Does This Article Contribute?

- Conditional deletion of the PTH1R in the vascular smooth muscle lineage causes increased cardiovascular fibrosis in the LDLR-deficient mouse model of diet-induced hyperlipidemia, diabetes, and arteriosclerosis.
- Novel hybrid serum response factor/monocyte enhancing factor 2 (Srf/Mef2) cognates are identified in *Col3a1* and *Col1a1* genes that mediate the inhibitor response to vascular smooth muscle PTH1R activity.
- Mkl1, a transcriptional co-adapter of Srf is shown to be negatively regulated by PTH1R signaling in vascular smooth muscle.
- Protein constituents of circulating extracellular vesicles are altered by the loss of vascular smooth muscle PTH1R and reflect pro-fibrotic Mkl1 signaling.
- Discovery of these connections may lead to strategies to monitor and mitigate cardiovascular complications in metabolic diseases where PTH1R signaling is altered.

The receptor for the bone anabolic hormones PTH and PTHrP is expressed throughout the arterial tree, but its role in cardiovascular disease is poorly characterized. Using Cre-loxP approaches, we conditionally deleted this receptor, the PTH1R, in the vascular smooth muscle (VSM) lineage in transgenic mice. We demonstrate that the PTH1R limits arterial fibrosis in the murine LDLR-deficient model of diet-induced diabetes, dyslipidemia, and arteriosclerosis. VSM PTH1R inhibits binding of Mkl1 to hybrid Srf/Mef2 cognates in the *Col3a1* and *Col1a1* genes, and PTH1R antifibrotic actions are mimicked by inhibition of Mkl1. Mass spectrometry demonstrates that the composition of circulating extracellular vesicles from LDLR−/− mice lacking VSM PTH1R is altered. Expression of one of these proteins, complement component 1 (C1r) is shown to be entrained to the VSM PTH1R--|Mk11 signal relay controlling *Col3a1* and *Col1a1*

expression. Discovery of this connection may lead to novel approaches to monitor and inhibit arterial fibrosis.

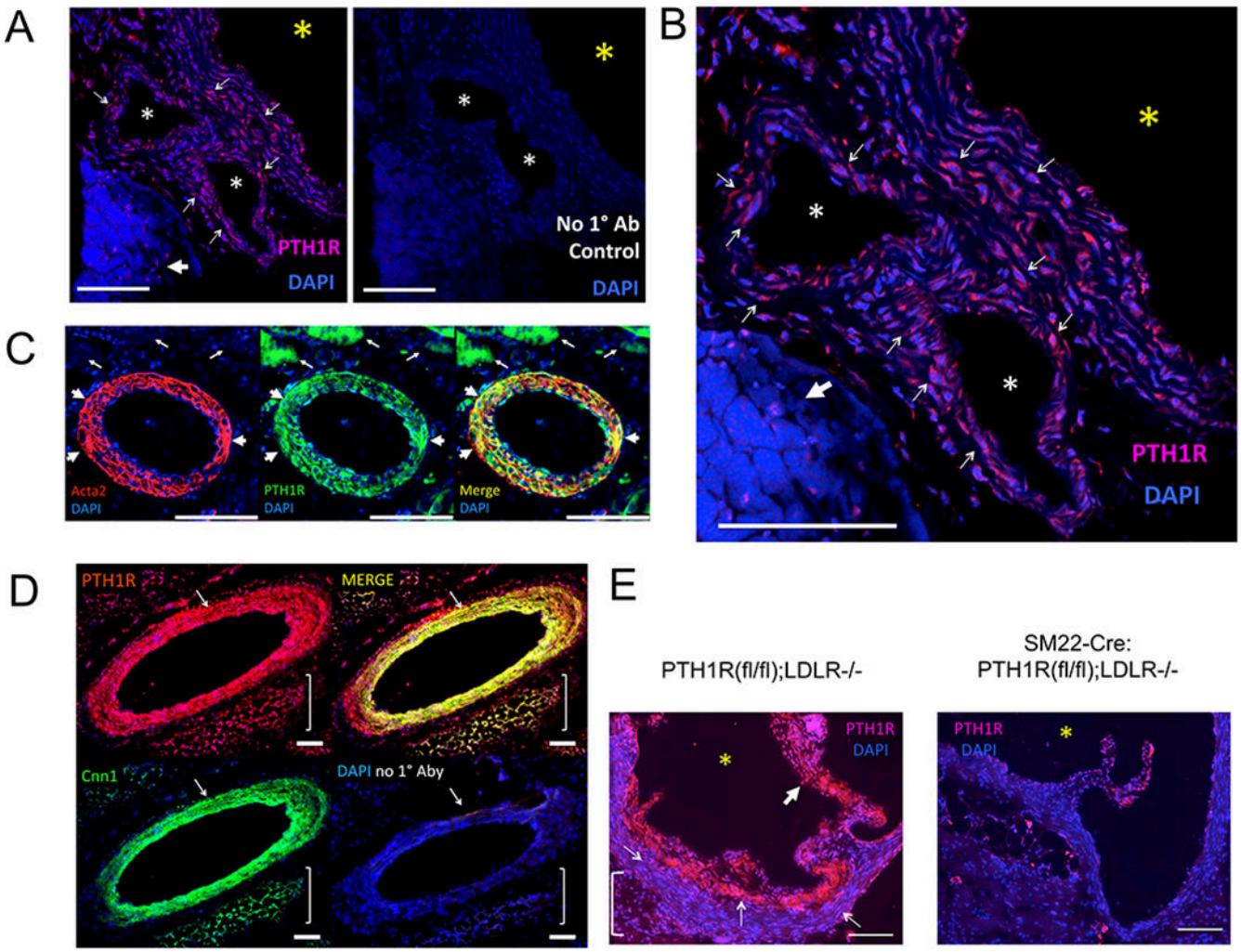

Figure 1: PTH1R protein accumulation is detected in arterial smooth muscle, and is decreased in SM22-Cre:PTH1R(fl/fl);LDLR−/− mice.

Panel A, in adult male LDLR−/− mice, PTH1R protein is visualized by confocal immunofluorescence in VSM cells within the media (white arrow) of aorta (yellow asterix) and coronary arteries. Little signal is seen in adjacent myocardium (white arrowhead). Panel B, higher magnification. Panel C, PTH1R protein was detected in medial VSM of interlobar arteries of the kidney, co-localizing (white arrowheads) with Acta2. PTH1R protein was also detected in adjacent renal tubules that do not express Acta2 (white arrows). Panel D, PTH1R protein is detected in the tunica media of mouse aorta, colocalizing with the VSM protein Cnn1 (white arrow). Colocalization of PTH1R with Cnn1 was also noted in the adjacent fibrofatty adventitia, indicating expression in microvascular pericytes or myofibroblasts. Panel E, aortic VSM, adventitial, and aortic valve interstitial PTH1R immunoreactivity is decreased in SM22-Cre:PTH1R(fl/fl);LDLR−/− mice vs. PTHR(fl/fl);LDLR−/− controls. Bracket, periaortic adventitia; thin arrows, aortic tunica media; thick arrow, aortic valve leaflet; yellow asterix, aortic lumen. Scale bar, 100 microns.

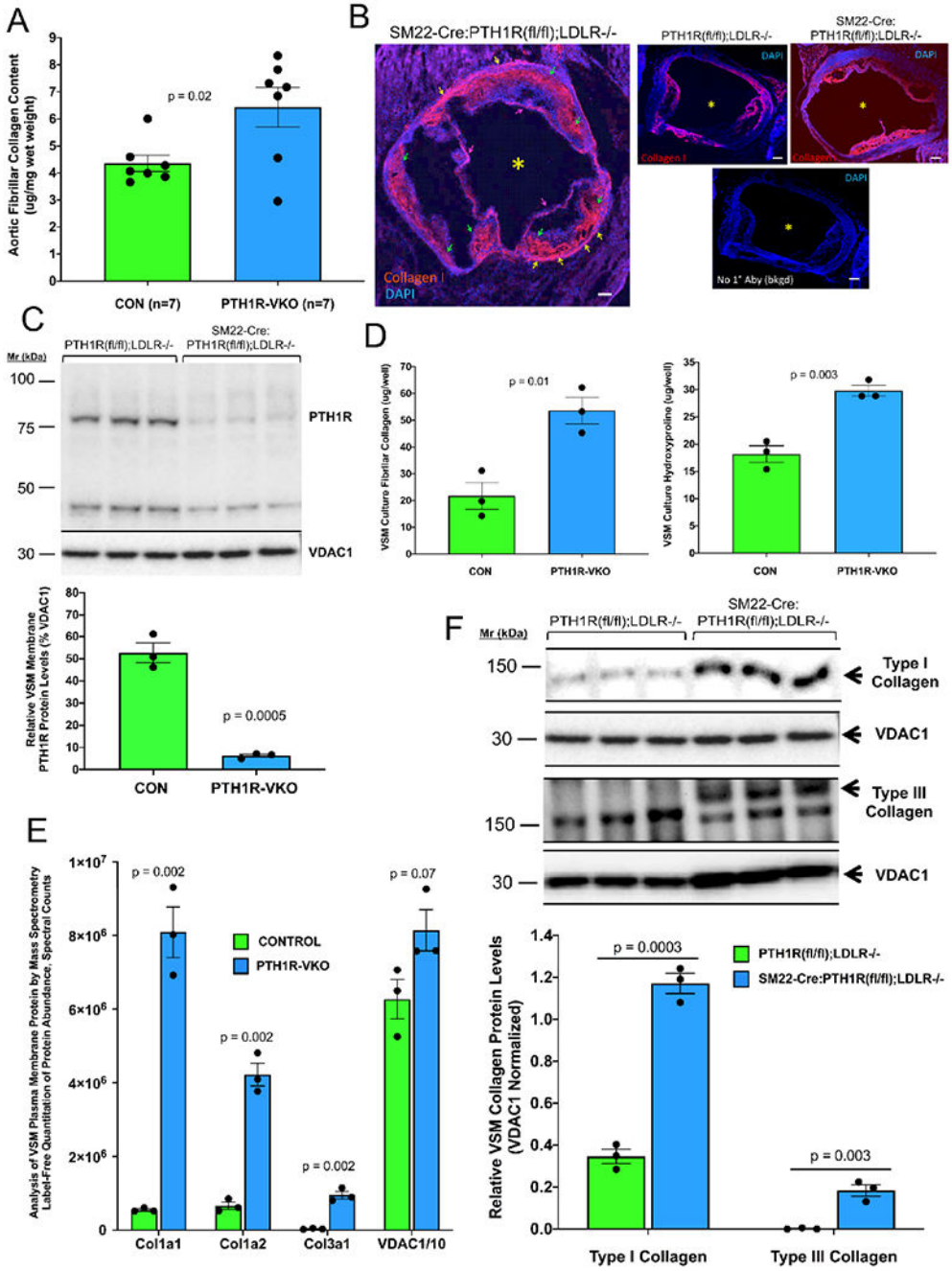

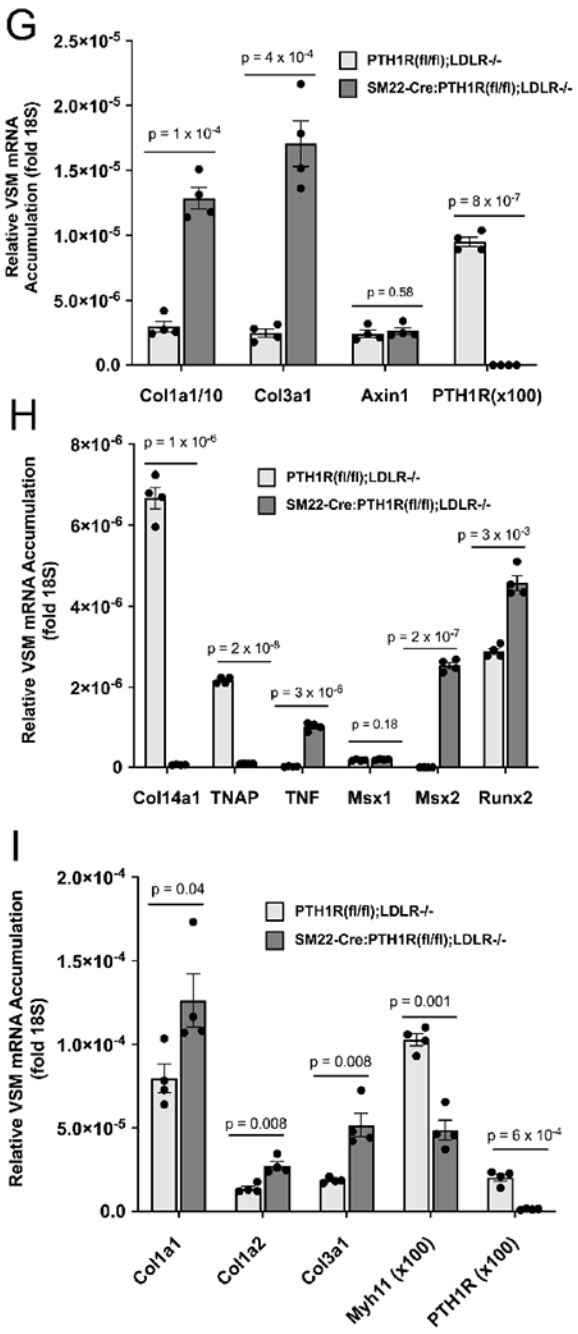

Figure 2: Fibrillar collagen accumulation is increased in SM22-Cre:PTH1R(fl/fl);LDLR−/− mice fed HFD as compared to PTH1R(fl/fl);LDLR−/− controls.

Male LDLR−/− mice of the indicated genotypes were fed HFD for 3 months beginning at 6 – 8 weeks of age. Thoracic aortic collagen was extracted and quantified, and aortic collagen visualized as in Methods. In parallel, primary aortic VSM were prepared from other cohorts for in vitro studies. Panel A, aortic collagen was significantly increased in SM22-Cre:PTH1R(fl/fl);LDLR−/− mice (PTH1R-VKO) vs. PTH1R(fl/fl);LDLR−/− controls (CON). Panel B, type I collagen accumulates in the media (yellow arrows), atheromas (green arrows), and valve leaflets (red arrows) in both SM22-Cre:PTH1R(fl/fl);LDLR−/−

and PTH1R(fl/fl);LDLR−/− cohorts. Histology confirm this fibrosis pattern including the adventitial-medial junction (Online Figure V). Panel C, western blot confirms PTH1R protein is decreased in extracts from SM22-Cre:PTH1R(fl/fl);LDLR−/− primary VSM. Panel D, collagen accumulation is increased in aortic VSM cultures from SM22-Cre:PTH1R(fl/fl);LDLR−/− mice vs. PTH1R(fl/fl);LDLR−/− controls, evident in Sircol (left panel) and hydroxyproline (right panel) assays. Panel E, aortic VSM cultures were prepared from male mice of the indicated genotypes. Plasma membrane extracts were prepared from independent triplicate cultures, partially resolved by SDS-PAGE (6.5 ug protein/sample), processed by in-gel proteolysis, and tryptic peptides analyzed and quantified by LC-MS/MS. Col1a1, Col1a2, and Col3a1 protein levels were significantly increased in aortic VSM cultures from SM22-Cre:PTH1R(fl/fl);LDLR−/− mice vs. controls. Panel F, western blot confirmed increases in type I and type III collagen with PTH1R deficiency. Lower panel, digital image analysis of western blot. Panel G, *Col1a1* and *Col3a1* mRNAs increased with VSM PTH1R deficiency. Panel H, *TNAP* and *Col14a1*, expressed in mineralizing osteoblasts, were decreased, even though other inflammatory osteogenic programs (TNF, Msx2, Runx2[1]) were upregulated. Panel I, siRNA targeting *PTH1R* in aortic VSM cultures upregulated *Col1a1* and *Col3a1*. *Myh11* was concomitantly reduced. N = 7 per genotype in panel A, n =3 per genotype all other panels. Statistical analyses panels A, C, and D: unpaired 2-tailed t-tests. Panels E-I: 2-tailed unpaired t-test, with Holm-Sidak adjusted p-values for multiple comparisons (4 comparisons panel E, 2 panel F, 4 panel G, 6 panel H, 5 panel I). Significant $p < 0.05$, nonsignificant $p > 0.05$ in all testing. All RT-qPCR analyses were repeated in at least one independent replicate experiment.

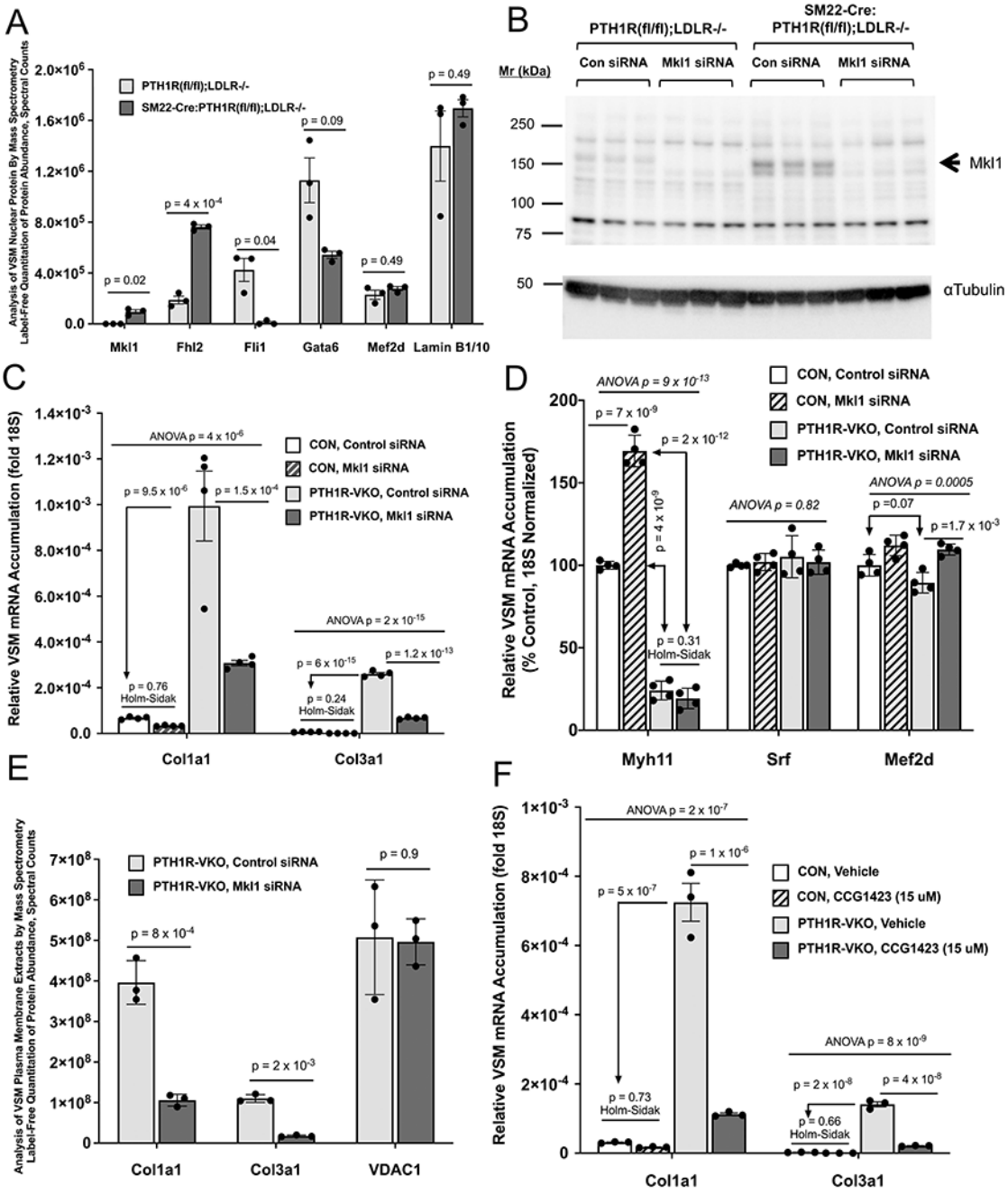

Figure 3: Mkl is increased in nuclear protein extracts prepared from SM22-Cre:PTH1R(fl/fl);LDLR−/− aortic VSM, and mediates Col1a1 and Col3a1 upregulation with VSM PTH1R deficiency.

Aortic VSM cultures were prepared from male mice of the indicated genotypes, and cultured as in Methods. Nuclear extracts were prepared from independent triplicate cultures, partially resolved by SDS-PAGE (8 ug/sample), processed by in-gel proteolysis, and tryptic peptides analyzed and quantified by LC-MS/MS. Panel A, LC-MS/MS revealed that nuclear Mkl1 and Fhl2 protein levels were significantly increased, while Fli1 and Gata6 levels were decreased, with VSM PTH1R deficiency. Lamin B1 and Mef2d were not altered. Panel B,

western blot confirmed upregulation of Mkl1 protein with PTH1R deficiency. Note that siRNA targeting *Mkl1* reduced Mkl1 protein levels. Panel C, siRNA targeting *Mkl1* profoundly inhibited upregulation of *Col1a1* and *Col3a1* mRNA accumulation in SM22-Cre:PTH1R(fl/fl);LDLR−/− (PTH1R-VKO) VSM cultures. Panel D, while *Srf* and *Mef2*, were unchanged, *Myh11* was reduced. Note that *Mkl1* siRNA increased *Myh11* mRNA in intact, but not in PTH1R –deficient VSM. Panel E, Mkl1 siRNA significantly reduced Col1a1 and Col3a1 protein levels (n = 3 / group, 16 ug protein/sample) in plasma membrane extracts from SM22-Cre:PTH1R(fl/fl);LDLR−/− VSM cultures. The housekeeping protein VDAC1 was not affected. Panels A, B, E, and F, n = 3 per group; panels C-D, n = 4 per group. Statistical analyses panels A and E: 2-tailed unpaired t-test, with Holm-Sidak adjusted p-values for multiple comparisons (6 comparisons panel A, 3 comparisons panel E). Panels C, D, and F: one-way ANOVA with Holm-Sidak adjusted p-values used in post-hoc testing to correct for multiple comparisons. All RT-qPCR analyses were repeated in at least one independent replicate experiment.

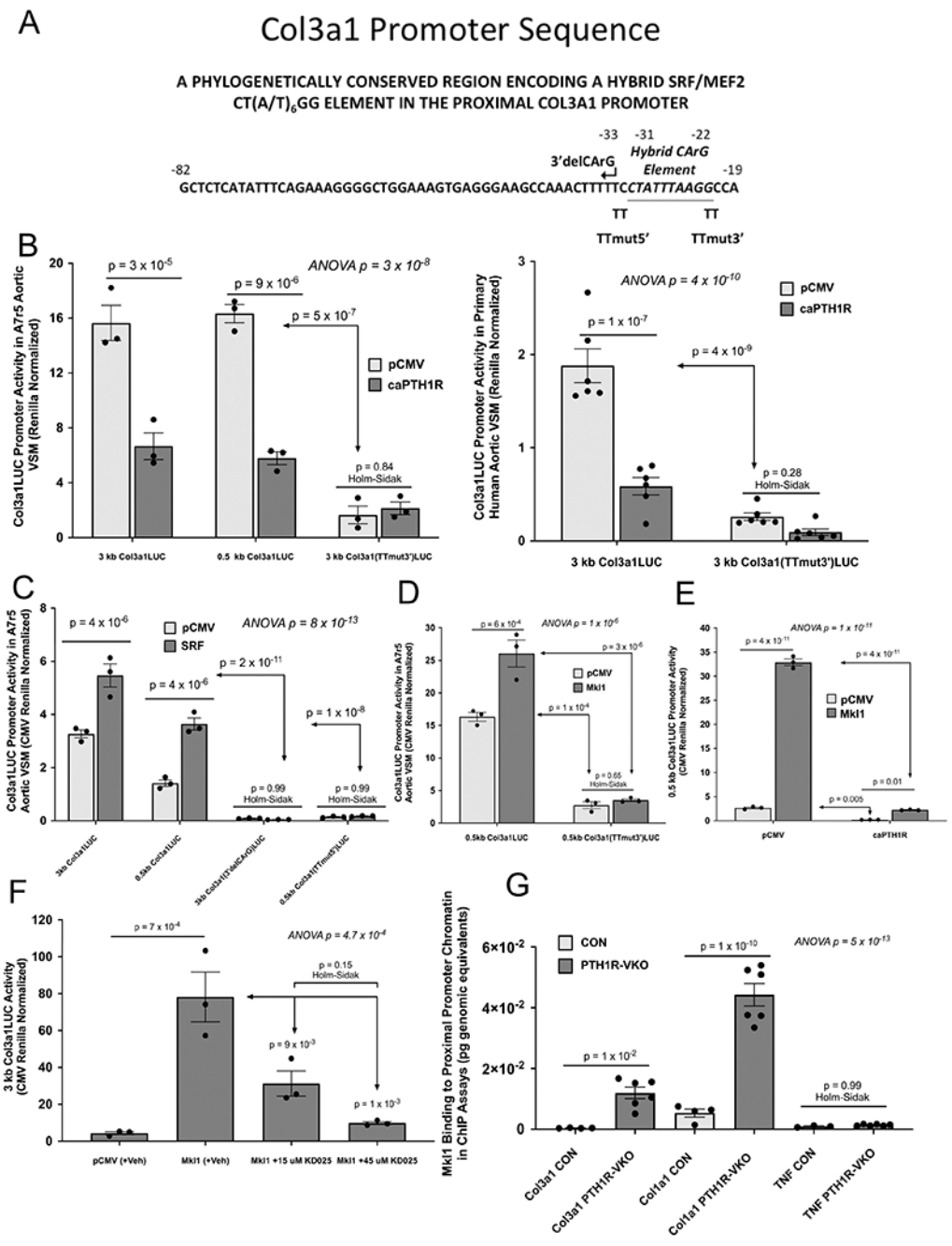

Figure 4: A hybrid Srf/Mef2 cognate in Col3a1 promoter conveys transcriptional responses to PTH1R and Mkl1.

Panel A, a 64 bp element in the proximal Col3a1 promoter is perfectly conserved between mice and humans. The hybrid[42] Srf/Mef2 cognate CT(A/T)6GG element is underlined. *Col3a1* promoter 3'-deletions and point mutations are also indicated. Numbering is per the mouse promoter[40]. Panel B, expression of the constitutively active PTH1R (caPTH1R[10, 44]) suppresses Col3a1 promoter activity in both A7r5 rat aortic VSM cells (left panel, n = 3 per group) and human primary aortic VSM cells (right panel, n = 6 per group). Dithymidine substitution in the 3'-region of the hybrid cognate, made within the context of the 3kb

Col3a1 promoter, reduces abolished significant caPTH1R regulation. Panel C, Srf activates the Col3a1 promoter, dependent upon the intact hybrid Srf/Mef2 cognate (n= 3 per group). Panel D, Mkl1 expression activates the Col3a1 promoter, dependent upon the intact hybrid cognate (n = 3 per group). Panel E, Col3a1 promoter activation is inhibited by co-expression of the caPTH1R (n = 3 per group). Panel F, the Rock2 kinase inhibitor reverses Mkl1 activation of the *Col3a1* promoter (n = 3 per group). Panel G, as compared to control (CON; n = 4 / group) Mkl1 binding to nuclear *Col3a1* and *Col1a1* proximal promoter chromatin is significantly increased with VSM PTH1R deficiency (PTH1R-VKO; n = 6 /group) as quantified by ChIP assay. The background ChIP signal at the *TNF* promoter was unaffected. Statistical analyses panels B-G: one-way ANOVA with Holm-Sidak adjusted p-values used in post-hoc testing to correct for multiple comparisons. All promoter analyses by luciferase assays were confirmed in at least 1 independent experiment.

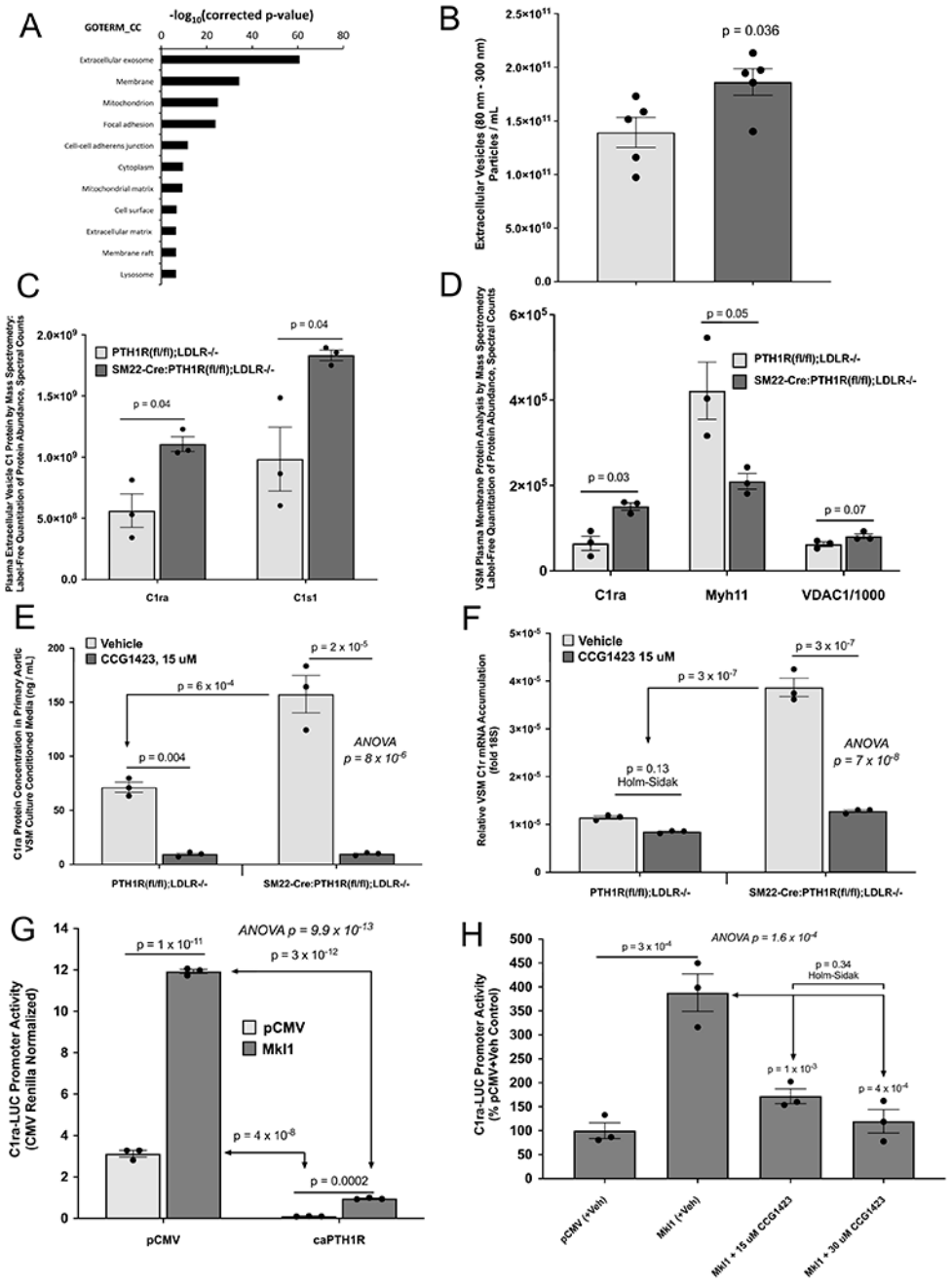

Figure 5: The complement protein C1ra is upregulated in circulating EVs from PTH1R-VKO mice, and reciprocally regulated by Mkl1 and PTH1R signaling in aortic VSM.

Primary aortic VSM cultures were prepared from male mice of the indicated genotypes. Plasma membrane extracts were prepared from independent triplicate cultures, partially resolved by SDS-PAGE, processed by in-gel proteolysis, peptides identified and quantified by LC-MS/MS, and analyzed using DAVID. **Panel A,** graphing of Gene Ontology (GO) terms vs. –log10(correct P) value, ranked from highest to lowest, for proteins significantly altered with PTH1R deficiency. Proteins involved with exosome biology were significantly represented. Panel B, EVs were isolated from fasting SM22-Cre:PTH1R(fl/fl);LDLR−/− and

PTH1R(fl/fl);LDLR−/− following 3 months HFD challenge, and characterized by nanoparticle tracking analysis (n =5 / genotype). EVs of 80–300 nm diameter were significantly increased with VSM PTH1R deficiency. Panel C, 10 ug of plasma EV protein prepared from individual animals (n = 3 per genotype) was analyzed by LC-MS/MS (Online Table IV). C1ra and C1s1 were significantly increased. Panel D, VSM membrane fractions (Figure 2E above) also exhibited significantly increased C1ra protein. Panel E, the Mkl1 inhibitor CCG1423 reduced C1ra protein accumulation in conditioned media of PTH1R-deficient VSM. Panel F, *C1ra* was upregulated in PTH1R-deficient VSM, and reduced by CCG1423. Panel G, the *C1ra* promoter is upregulated by Mkl1, and inhibited by caPTH1R in HEK293T cells. Panel H, upregulation of C1ra promoter activity by Mkl1 in A7r5 VSM is inhibited by the Mkl1 inhibitor CCG1423. Panel B, n = 5 / genotype as shown. Panels C – H, n = 3 per group. Statistical analyses panels B - D: 2-tailed unpaired t-tests, with Holm-Sidak adjusted p-values for multiple comparisons (1 comparison panel B, 2 comparisons panel C, 3 comparisons panel D). Panels E-H: one-way ANOVA with Holm-Sidak adjusted p-values used in post-hoc testing to correct for multiple comparisons.

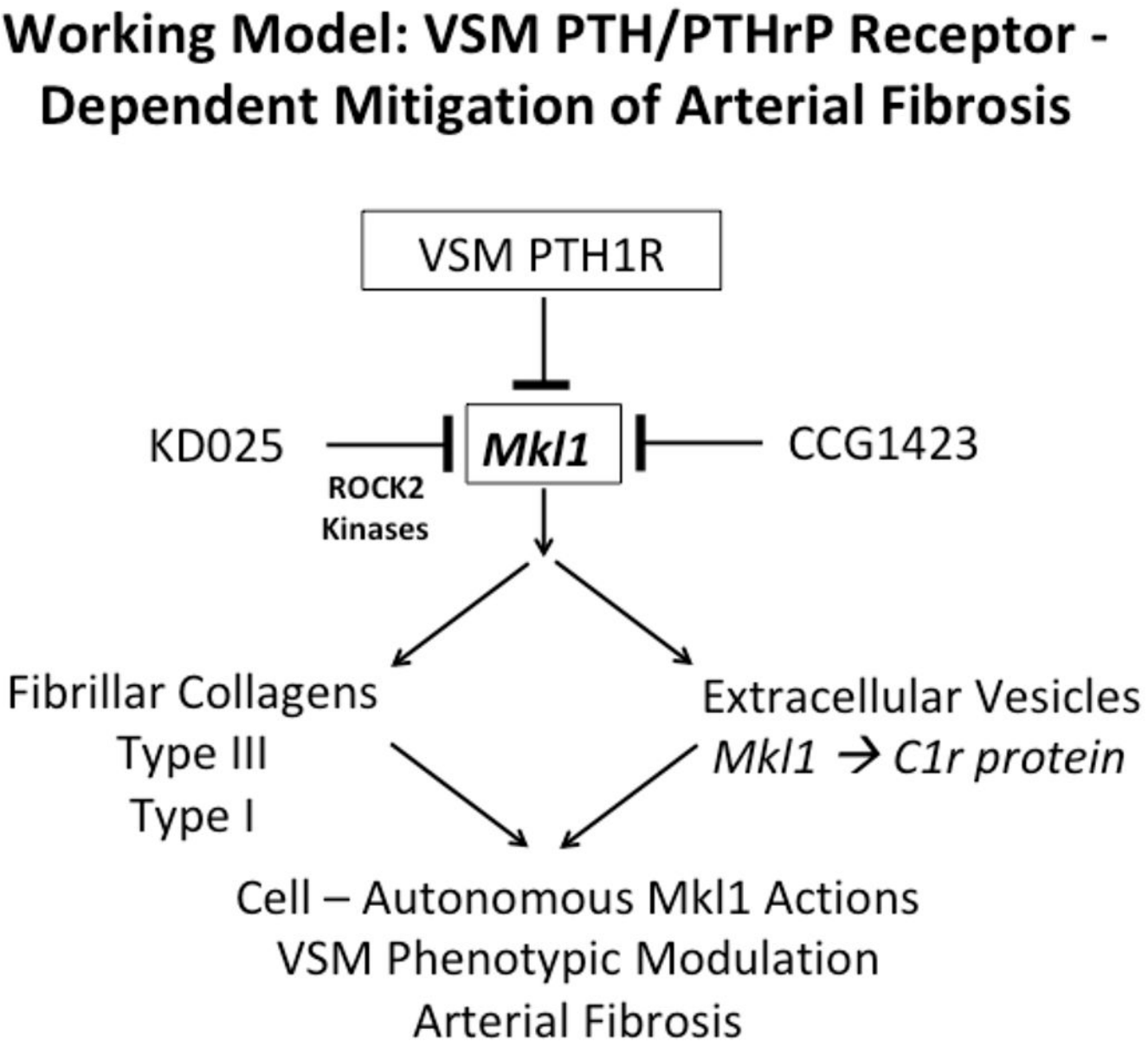

Figure 6: A working model for VSM PTH1R –dependent mitigation of arterial fibrosis.

In a cell-autonomous fashion, endogenous PTH1R activity restrains Mkl1 expression and activity that supports VSM collagen expression via novel hybrid[42] MADS-box elements. Changes in VSM PTH1R signaling tone, mediated in part by Mkl1 modulation, are reflected in circulating EV C1r protein and EV-mediated osteogenic gene regulation. The mechanisms whereby PTH1R deficiency uncouples fibrosis vs. osteogenic mineralization, while supporting VSM contractile phenotype, remain to be determined -- but likely involve dysregulated Srf/Mkl1 actions[66] that reduce expression of differentiation-specific genes (myogenic and osteogenic) while driving fibrosis during VSM phenotypic modulation. Strategies that directly (CCG1423) or indirectly (KD025) inhibit cell-autonomous Mkl1

actions are predicted to mitigate arterial fibrosis arising from impaired PTH1R signaling[18, 54, 56].